Cyclopolymerization Reactions of Diallyl Monomers: Exploring Electronic and Steric Effects Using DFT Reactivity Indices

İlke Uğur,[†] Freija De Vleeschouwer,[‡] Nurcan Tüzün,[§] Viktorya Aviyente,[†] Paul Geerlings,[‡] Shubin Liu,[||] Paul W. Ayers,[⊥] and Frank De Proft*[,‡]

Chemistry Department, Faculty of Arts and Sciences, Boğaziçi University, 34342 Bebek, Istanbul, Turkey, Eenheid Algemene Chemie, Faculteit Wetenschappen, Vrije Universiteit Brussel, Pleinlaan 2, 1050 Brussels, Belgium, Chemistry Department, Faculty of Science and Letters, Istanbul Technical University, 34469 Maslak, Istanbul, Turkey, Research Computing Center, University of North Carolina, 211 Manning Drive, Chapel Hill, North Carolina 27599-3420, Department of Chemistry, McMaster University, Hamilton, Ontario, Canada L8S 4M1

Received: April 12, 2009

The regioselectivity in the cyclopolymerization of diallyl monomers is investigated using DFT-based reactivity indices. In the first part, the experimentally observed mode of cyclization (exo versus endo) of 11 selected radicals involved in this process is reproduced by the computation of activation energies, entropies, enthalpies, and Gibb's free energies for the 5- and 6-membered cyclization reactions. The application of a recently proposed energy partitioning of the activation barriers shows that the regioselectivity cannot be explained by the steric effect alone. Next, a number of relevant DFT-based reactivity indices, such as non-spin-polarized and spin-polarized Fukui functions, spin densities, and dual descriptors, were applied to probe the role of the polar and stereoelectronic effects in this reaction. The dual descriptor has been found to reproduce best the experimental trends, confirming the important role of the stereoelectronic effects.

1. Introduction

Allyl monomers are known as poor monomers to yield high molecular weight polymers via polymerization reactions.[1] The abstraction of the reactive allylic hydrogen of the monomer causes chain transfer reactions, which yield decreased molecular weight polymers.[2] Although allyl compounds are not good monomers for polymerization, their difunctional analogues can be polymerized through cyclopolymerization (Scheme 1). Butler's discovery of polymerizations of diallyl compounds, later named "cyclopolymerizations", made it possible to synthesize high molecular weight water-soluble polymers from diallyl monomers.[3−5] Because of their properties, these cyclopolymers are suitable for a wide range of industrial applications.

The cyclopolymerization reaction of the diallyl monomers starts with the initiation of the diallyl molecule, creating a radical center, which is followed by the cyclization reaction which is the focus of this contribution. The intramolecular cyclization reactions give two possible products with two possible repeating units. The repeating cyclization units can be 5-membered-exo- or 6-membered-endo-cyclic structures, depending on the regioselectivity of the radical addition to the double bond (Scheme 1). Next, the cyclized radical reacts with another monomer, and the polymerization proceeds; this is called intermolecular propagation as depicted in Scheme 1.

In this study, the regioselectivity in this first radical cyclization step of the cyclopolymerization reactions of the diallyl compounds, yielding 5- or 6-membered cyclic monomers, will be investigated using DFT reactivity indices (Scheme 2). Monomers

SCHEME 1: Cyclopolymerization Reactions of Diallyl Monomers Considered in This Study[a]

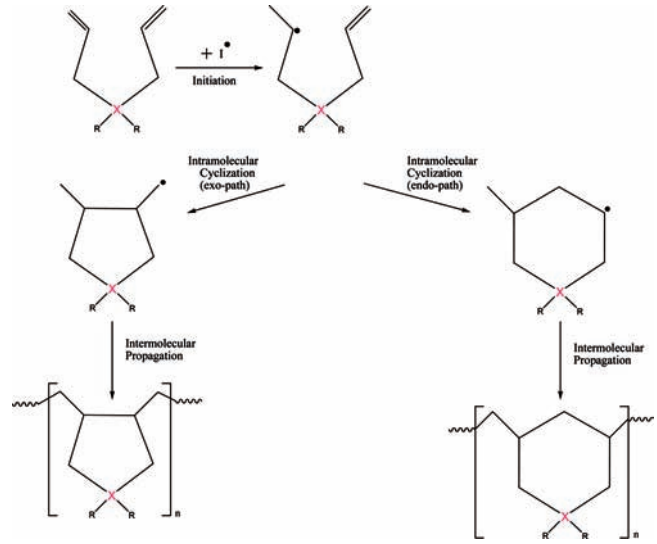

[a] X = N, O; R = H, CH_3, lone pair; I = initiator.

M1−**M8**, (**M1** = *N*-methyl-*N*,*N*-diallylammonium, **M2** = *N*,*N*-diallylamine, **M3** = *N*,*N*-dimethyl-*N*,*N*-diallylammonium, **M4** = *N*-methyl-*N*,*N*-diallylamine, **M5** = *N*,*N*-dimethyl-*N*,*N*-diallylammonium, **M6** = *N*-methyl-*N*-allyl-2-(methoxycarbonyl)-allylamine, **M7** = diallyl ether, **M8** = methyl α-(allyloxymethyl)acrylate) are known to cyclopolymerize to yield polymers with 5-membered ring units. **M9**, **M10**, and **M11** (**M9** = *N*-methyl-*N*-methallyl-2-(methoxycarbonyl)allylamine, **M10** = methyl α-hydroxymethlacrylate, **M11** = α-(2-phenylallyloxy)-methylstyrene) are known to cyclopolymerize to yield polymers with 6-membered ring units. In our earlier studies, the exo vs

* Corresponding author. E-mail: fdeprof@vub.ac.be.
[†] Boğaziçi University.
[‡] Vrije Universiteit Brussel.
[§] Istanbul Technical University.
[||] University of North Carolina.
[⊥] McMaster University.

10.1021/jp903371b CCC: $40.75
Published on Web 07/01/2009

SCHEME 2: Structures of the Different Diallyl Monomers Investigated in the Present Work

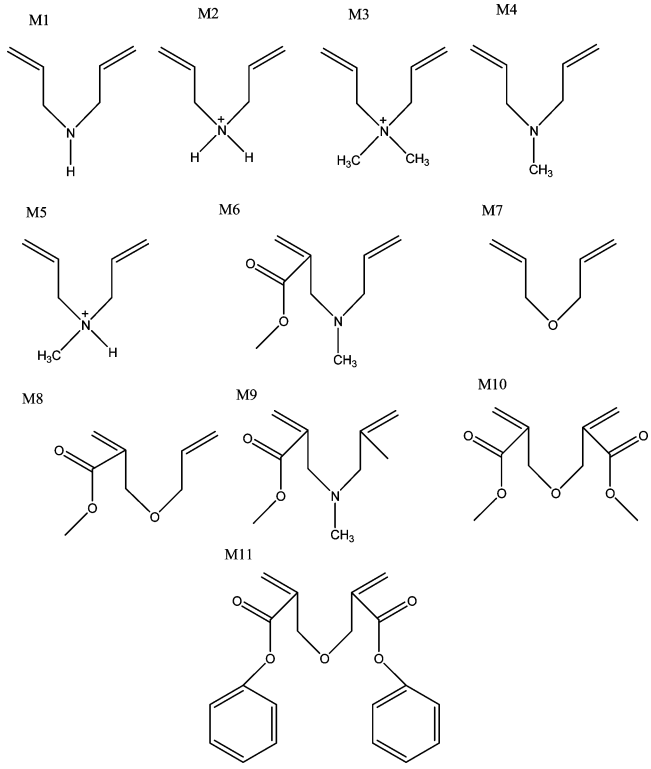

endo preferences of the models were rationalized on the basis of steric, stereoelectronic, polar, and entropic effects.[6−9] The calculated thermochemical parameters such as activation entropies, enthalpies, and free energies for the cyclization reactions have been found to be in agreement with experiment.[6−9] An NBO analysis on diallyl ether and methyl α-[(allyloxy)methyl]acrylate has indicated that the regioselectivity may be sensitive to hyperconjugative interactions.[7]

In the present contribution, various descriptors, defined within the framework of density functional theory (DFT), are used to explain the regioselectivity of the radical cyclizations preceding the intermolecular propagation step in the cyclopolymerization reactions. The transition states and the activation barriers for both the exo and the endo modes of the cyclization for a number of diallyl radicals, depicted in Scheme 3, are determined. An alternative and recently introduced energy decomposition of the activation barriers is used to investigate the steric effect in the cyclizations. Next, the non-spin-polarized and spin-polarized Fukui functions for a radical attack on the radical conformer minima close to the transition state are computed, in analogy with an earlier study of De Proft et al.[10,11] The reactive conformations of the radicals (designated as the reactive rotamers, not the structures corresponding to the global minima) are used for the calculation of the reactivity indices.[12] The 3D structures corresponding to the reactive rotamers of monomers **M1**−**M11** can be found in Scheme 3. To gain a more detailed insight into the polar factors controlling the exo vs endo mode of cyclization, the Fukui functions were investigated along the reaction path in the case of two prototypical cyclization reactions for **R4** and **R10**. Finally, the spin-polarized dual descriptor of the radicals is computed and plotted to investigate stereoelectronic effects on the regioselectivity.

2. Theory and Computational Details

Different effects influencing the regioselectivity of the cyclization of the radicals derived from diallyl radicals will be investigated using concepts introduced in DFT based reactivity theory ("conceptual DFT").[13] A central quantity often used in studies of regioselectivity is the Fukui function $f(\underline{r})$ introduced by Parr and Yang and defined as the initial response of the electron density due to an infinitesimal perturbation in the total number of electrons N, at constant external potential $v(\underline{r})$[14,15]

$$f(\underline{r}) = \left(\frac{\partial \rho(\underline{r})}{\partial N}\right)_v \tag{1}$$

Due to the discontinuity of the electron density with respect to the number of electrons,[16,17] three different Fukui functions can be introduced, representing the case of a nucleophilic attack, $f^+(\underline{r})$; an electrophilic attack, $f^-(\underline{r})$; or a neutral (radical) attack, $f^0(\underline{r})$. For a system of N electrons, these can be computed as

SCHEME 3: Structures of the Radicals of the Selected Diallyl Monomers Investigated in the Present Work

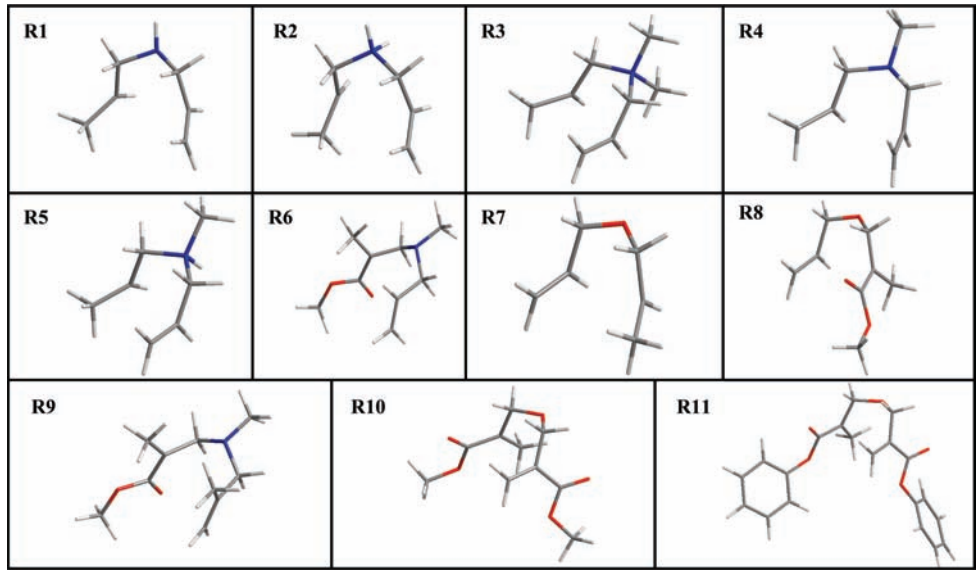

$$f^{+}(\underline{r}) = \rho_{N+1}(\underline{r}) - \rho_{N}(\underline{r}) \quad (2)$$

$$f^{-}(\underline{r}) = \rho_{N}(\underline{r}) - \rho_{N-1}(\underline{r}) \quad (3)$$

and

$$f^{0}(\underline{r}) = \frac{f^{+}(\underline{r}) + f^{-}(\underline{r})}{2} \quad (4)$$

that is, the average of the Fukui functions for an electrophilic and a nucleophilic attack. In these equations, $\rho_{N+1}(\underline{r})$, $\rho_{N}(\underline{r})$, and $\rho_{N-1}(\underline{r})$ represent the electron densities of the $N + 1$, N, and $N - 1$ electron system computed at the geometry of the N electron system. High values of these quantities imply high probabilities of a nucleophilic, electrophilic, or radical attack, respectively. The derivative of the Fukui function with respect to the number of electrons is the so-called dual descriptor of chemical reactivity, $f^{(2)}(\underline{r})$.[18]

$$f^{(2)}(\underline{r}) = \left(\frac{\partial f(\underline{r})}{\partial N}\right)_{v} \approx f^{+}(\underline{r}) - f^{-}(\underline{r}) \quad (5)$$

Among other things, the dual descriptor is useful for casting the famous Woodward−Hoffmann rules for pericyclic reactions in conceptual DFT.[19] $f^{(2)}(\underline{r})$ will be positive in regions of a molecule that are better at accepting electrons than they are at donating electrons, whereas $f^{(2)}(\underline{r})$ will be negative in regions that are better at donating electrons than they are at accepting electrons. It is then stated that favorable chemical reactions occur when regions that are good electron acceptors ($f^{(2)}(\underline{r}) > 0$) are aligned with regions that are good electron donors ($f^{(2)}(\underline{r}) < 0$).[18,19]

To gain insight into the global electrophilic nature, we have also computed the global electrophilicity index of these radicals, a quantity that was introduced by Parr et al.[20,21] as

$$\omega = \frac{\mu^2}{2\eta} \quad (6)$$

where μ is the electronic chemical potential[22] and η is the chemical hardness.[23−25] This quantity was computed using a finite difference approximation for μ and η[20] as

$$\omega \approx \frac{(I + A)^2}{8(I - A)} \quad (7)$$

where I and A are the vertical ionization energy and electron affinity, respectively.

All of these chemical concepts can be generalized in the framework of the so-called spin-polarized conceptual DFT;[26] in this representation, changes from one ground state to another are written in terms of the changes of N, v, and N_s, the spin number which is the difference between the number of α- and β-spin electrons. (An equivalent representation uses N_α, N_β, and v[26b,c,27]). In this framework, the Fukui function, f_{NN}, can be written as[26,27]

$$f_{NN}(\underline{r}) = \left(\frac{\partial \rho(\underline{r})}{\partial N}\right)_{N_s,v} \quad (8)$$

which can be proven to be equal to[27]

$$f_{NN}(\underline{r}) = \frac{1}{2}[f_{\alpha\alpha}(\underline{r}) + f_{\alpha\beta}(\underline{r}) + f_{\beta\alpha}(\underline{r}) + f_{\beta\beta}(\underline{r})] \quad (9)$$

The Fukui functions in the $\{N_\alpha, N_\beta, v\}$ representation are defined as follows:

$$f_{\alpha\alpha}(\underline{r}) = \left(\frac{\partial \rho_\alpha(\underline{r})}{\partial N_\alpha}\right)_{N_\beta,v} \qquad f_{\alpha\beta}(\underline{r}) = \left(\frac{\partial \rho_\alpha(\underline{r})}{\partial N_\beta}\right)_{N_\alpha,v}$$
$$f_{\beta\alpha}(\underline{r}) = \left(\frac{\partial \rho_\beta(\underline{r})}{\partial N_\alpha}\right)_{N_\beta,v} \qquad \text{and } f_{\beta\beta}(\underline{r}) = \left(\frac{\partial \rho_\beta(\underline{r})}{\partial N_\beta}\right)_{N_\alpha,v} \quad (16)$$

where ρ_α (ρ_β) is the density of the α (β)-electrons. The Fukui function for a radical attack is the average of the Fukui functions for a nucleophilic and an electrophilic attack:

$$f^{0}_{NN}(\underline{r}) = \frac{f^{+}_{NN}(\underline{r}) + f^{-}_{NN}(\underline{r})}{2} \quad (10)$$

In addition, spin-polarized versions of the dual descriptor have been put forward recently.[26b,28]

To gain insight into the influence of the steric effect on the barriers of the exo- and endo-cyclization, we have performed an analysis along the lines introduced by one of us, writing the energy as[29]

$$E \equiv E_s + E_e + E_q \quad (11)$$

where E_s, E_e and E_q are the steric, electrostatic and quantum contributions to the energy.[41] This expression can then be compared with the energy expression from density functional theory,

$$E[\rho] = T_s[\rho] + V_{ne}[\rho] + J[\rho] + V_{nn}[\rho] + E_{xc}[\rho] \quad (12)$$

where $T_s[\rho]$, $V_{ne}[\rho]$, $J[\rho]$, $V_{nn}[\rho]$, and $E_{xc}[\rho]$ represent the noninteracting kinetic, nucleus-electron attraction, classical electron−electron repulsion, nucleus−nucleus repulsion and exchange-correlation energies, respectively. Terms 2, 3, and 4 of this expression are electrostatic in nature, so one can write that

$$E_e = V_{ne}[\rho] + J[\rho] + V_{nn}[\rho] \quad (13)$$

The quantum contribution to the energy is due to the exchange-correlation energy and a contribution to the kinetic energy, which is defined as the difference of $T_s[\rho]$ and $T_W[\rho]$, the Weizsäcker kinetic energy, given as follows:

$$T_W[\rho] = \frac{1}{8}\int \frac{|\nabla \rho(\underline{r})|^2}{\rho(\underline{r})}\, d\underline{r} \quad (14)$$

Combining both equations yields the following definition of the steric energy:

$$E_s \equiv T_W[\rho] \quad (15)$$

TABLE 1: Energetics for Cyclization of the Radicals (kcal/mol)[a]

	$\Delta E^{\neq}$ (gas)		$\Delta E^{\neq}$ (DMSO)		$\Delta H^{\neq}$		$\Delta G^{\neq}$	
radical	$\Delta E^{\neq}$ (exo)	$\Delta E^{\neq}$ (endo)	$\Delta E^{\neq}$ (exo)	$\Delta E^{\neq}$ (endo)	$\Delta H^{\neq}$ (exo)	$\Delta H^{\neq}$ (endo)	$\Delta G^{\neq}$ (exo)	$\Delta G^{\neq}$ (endo)
R1	6.8	10.8	6.9	10.7	5.8	9.7	8.9	12.9
R2	6.6	9.8	5.1	9.2	5.6	8.7	8.6	11.9
R3	4.5	8.8	4.0	8.6	3.6	7.9	6.0	10.4
R4	4.7	10.3	4.8	10.1	3.8	9.3	6.4	12.1
R5	5.2	9.1	3.8	8.9	4.3	8.2	7.0	11.0
R6	8.9	12.5	9.0	12.6	8.0	11.5	10.9	14.6
R7	5.7	10.8	5.7	11.0	4.7	9.7	8.0	13.5
R8	10.0	12.9	9.8	12.9	9.1	11.9	12.1	15.3
R9	13.8	11.0	14.0	10.6	12.9	10.1	16.0	12.9
R10	13.9	8.7	16.2	8.7	13.0	7.8	17.4	11.7
R11	15.2	8.7	15.7	8.6	14.5	7.8	18.0	11.5

[a] B3LYP/6-311++G(d,p), $T = 298.15$ K for $\Delta G^{\neq}$ and $\Delta H^{\neq}$.

TABLE 2: Activation Entropies for Cyclization Reactions (cal/mol K)[a]

	$\Delta S^{\neq}$		$\Delta\Delta S^{\neq}$
radical	$\Delta S^{\neq}$ (exo)	$\Delta S^{\neq}$ (endo)	$\Delta S^{\neq}$ (exo) − $\Delta S^{\neq}$ (endo)
R1	−10.11	−10.64	0.52
R2	−10.08	−10.73	0.64
R3	−7.88	−8.51	0.62
R4	−8.78	−9.3	0.52
R5	−8.79	−9.34	0.55
R6	−9.6	−10.48	0.88
R7	−11.29	−12.77	1.47
R8	−10.19	−11.34	1.15
R9	−10.43	−9.3	−1.13
R10	−14.83	−13.28	−1.54
R11	−11.81	−12.42	0.61

[a] B3LYP/6-311++G(d,p).

TABLE 3: Differences of the Steric ΔE_s, Electrostatic ΔE_e, and Quantum ΔE_q Energy Contributions to the Transition Structures of the Exo and Endo Modes of Cyclization for the Different Radicals[a]

radical	ΔE_s	ΔE_e	ΔE_q
R1	−9.2	−4.6	9.9
R2	−10.2	−2.5	9.5
R3	−3.5	−5.0	4.2
R4	−4.5	−6.6	5.6
R5	−11.1	−2.9	10.1
R6	20.5	−5.5	−18.1
R7	3.0	−7.1	−0.9
R8	16.9	−3.5	−16.0
R9	17.6	4.2	−18.8
R10	−39.5	13.9	31.3
R11	−2.9	11.6	−1.5

[a] These values are obtained as the differences of these quantities of the exo and endo transition structures. All values were obtained at the B3LYP/6-311++G(d,p) level of theory and are in kcal/mol.

The definition of the steric energy in eq 15 has proved effective for understanding internal rotation and transition state barriers;[30] it also makes contact with recent work on understanding chemical reactivity using the principles of information theory.[30]

All calculations (ground state structure optimizations, transition state optimizations, IRC calculations, and electronic properties) were performed at the B3LYP[31]/6-311++G(d,p)[32] level of theory using the Gaussian 03 program.[33] The energy partitioning presented above was carried out at the same level of theory. Atomic electron populations and spin densities were obtained within the NPA scheme.[34] The effect of a polar environment on the reaction path has been taken into account by use of the self-consistent reaction field theory. Single-point energies in DMSO making use of the integral equation formalism-polarizable continuum model[35−38] at the B3LYP/6-311++G(d,p) level of theory have been performed.

3. Results and Discussions

a. Energetics and the Entropic Effect. Experimental polymerization studies carried out on compounds **R1**−**R11** have shown that the radicals **R1**−**R8** form exclusively five-membered rings in their polymer backbones, whereas radicals **R9**−**R11** form six-membered ring structures.[11,39,40]

When the energetics of activation of the cyclopolymerization reaction are considered (Table 1), for the radicals that undergo exo-cyclization (**R1**−**R8**), the exo mode of cyclization has a lower activation barrier than the endo mode. For the radicals that undergo endo-cyclization (**R9**−**R11**), the trend reverses. The enthalpy and free energy of activation follow the same trend (Table 1). Note that zero-point energies are included in all the values. This trend survives when the solvent is included in the calculations via the use of a continuum model. In this study, because all model monomers and their polymers are water-soluble, dimethylsulfoxide (DMSO) is chosen as a polar solvent with a dielectric constant $\varepsilon = 48$. It is also one of the solvents that have been used for the cyclopolymerization reactions of diacrylamide,[41] methacrylic anhydride,[42] diallylamine hydrochloride with sulfur dioxide,[43] DADMAC with sulfur dioxide,[44] and some diallylamine derivatives.[45] As seen in Table 1, the energy barriers are consistent with the experimental observations.

The contribution of entropy to the regioselectivity has also been investigated because the unexpected exo preference of hexenyl systems has been attributed to a favorable activation entropy in the literature.[46] The entropies of activation of the exo- vs endo-cyclizations considered in this work are listed in Table 2. Indeed, the entropy of activation for the cyclization of **R1**−**R8** is lower in the exo mode than in the endo mode. This trend is reversed for **R9** and **R10**, but not for **R11**. Except for the **R11**, all the radicals entropically favor the experimental pathway. Although the trend is consistent with the experimental ring size preference, the $\Delta\Delta S^{\neq}$ values are less than 1.15 (cal/(mol K)) which is far too small to be the dominant factor for the regioselectivity.

b. Energy Partitioning of the Activation Barriers: Steric Effect. In Table 3, we list the differences of the three contributions, E_s, E_e, and E_q for the transition structures of the exo and endo modes of cyclization.

From the data in Table 3, it can be concluded that the barrier heights of these reactions do not appear to be governed by the steric effect, in the sense that it was defined above, since no

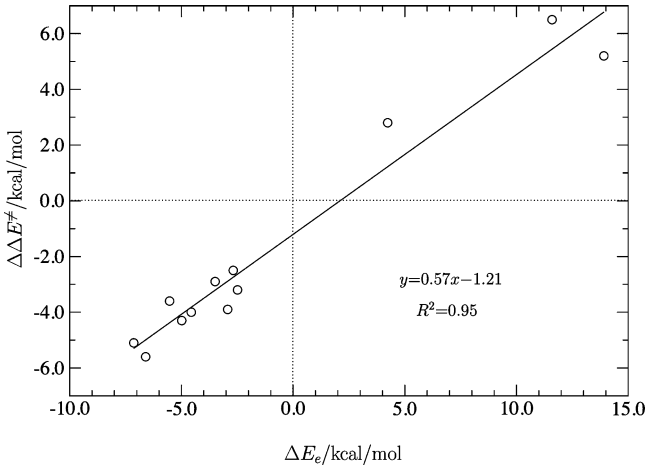

Figure 1. Correlation of the difference of the activation barrier of the exo and the endo mode, $\Delta\Delta E^{\neq} \equiv \Delta E^{\neq}_{exo} - \Delta E^{\neq}_{endo}$, of cyclization with the electrostatic contribution difference ΔE_e of the transition state energies.

correlation exists between these differences and the reaction barrier differences. However, there appears to be a good linear relationship between the barrier differences and the electrostatic contribution, as can be seen from the plot given in Figure 1. In the next section, we will thus attempt to gain insight into the observed regioselectivities using a number of local reactivity indices.

c. Polar and Stereoelectronic Effects: Reactivity Indices. We will now investigate the regioselectivity of the cyclizations of the diallylmonomers central in this work using reactivity indices emerging from density functional theory. In the first part, the polar and stereoelectronic effects and their role in explaining the observed regioselectivity will be examined. The global electrophilicities of the radicals, the Fukui functions for radical attack (both non-spin- and spin-polarized), and the spin densities on the relevant atoms in the cyclization process were calculated for all radicals. For each radical, the indices are tabulated for three atoms: for the carbon bearing the radical center, the exo carbon (the carbon atom on the double bond that will form a 5-membered ring upon cyclization), and the endo carbon (the carbon atom on the double bond that will form a 6-membered ring upon cyclization). The global electrophilicity values for all radicals indicate that these can be classified as being nucleophilic to neutral,[47] except for high values associated with the radical cations **R2**, **R3**, and **R5** (Table 4). These electrophilicity values thus point to an interaction between the SOMO of the nucleophilic radical and the LUMO of the relevant carbon with the double bond.[45]

For all cases considered in this work, the Fukui functions are highest on the radical center, which is the most reactive carbon. The second highest Fukui function values are on the endocarbon atoms for all radicals, and the lowest values are on the exocarbon atoms. Although the numerical values of these two quantities differ, this is the case for both the non-spin-polarized (f^0) and the spin-polarized (f^0_{NN}) Fukui functions. This fact shows that the Fukui functions favor the thermodynamic product, that is, the formation of the six-membered ring.

Close inspection of the spin density shows that the radical center and the endo carbon have an excess of alpha spin and the exo carbon has an excess of beta spin. If spin-coupling between centers of opposite spin controlled the reactivity, then all radicals would undergo cyclization in the exo mode.

Insight into the observations made for the Fukui functions is obtained when considering the evolution of this quantity along the reaction path; we plot in Figure 2 the evolution of f^0_{NN} along the reaction profile for the endo-cyclization mode for radical **R10** (a compound with a preferred endo regioselectivity of cyclization) and the exo-cyclization mode for radical **R4** (a compound with a preferred exo regioselectivity of cyclization). For the endo mode (IRC calculations starting from endo transition state) of the radicals (Figure 2a), we observe that the Fukui function is initially always the highest on the radical center; the second highest value initially occurs on the endo carbon, whereas the exo carbon initially has the lowest value. During the reaction, the radical atom loses its reactivity, and the exo carbon gains the reactivity. At the end of the reaction, the exo carbon is the one with the highest reactivity, which is meaningful, since it is the new radical center for an endo-cyclization path. When an exo-cyclization is considered (Figure 2b), at the beginning of the reaction, the radical center again has the highest value. The second highest value of the Fukui function is on the endo carbon, and the exo carbon has the lowest value. Since it is an exo pathway, the second reactive carbon atom is supposed to be the exo carbon at the beginning of the reaction. So we can say that we do not have the correct information about the regioselectivity at the beginning of the reaction for the exo pathway. However, during the reaction, the reactivity of the endo carbon increases, and at the end of the reaction, the endo carbon becomes the highest reactive carbon atom, which is again meaningful, since the endo carbon is the new radical center for the exo case. Furthermore, for the endo case (Figure 2a), the Fukui function on the exo carbon becomes larger than the endo carbon, only very close to the transition state. This points to the fact that this transition state occurs much later than the exo transition state.[41] This is supported by the distance between the radical carbon and the exo carbon of the exo transition state geometry and the distance

TABLE 4: Reactivity Indices: Global Electrophilicity (GE), Fukui Function (f^0), Spin-Polarized Fukui Function (f^0_{NN}), Spin Density (ρ_s) (B3LYP/6-311++G(d,p))

		f^0			f^0_{NN}			ρ_s		
radicals	GE	exo C	endo C	radical C	exo C	endo C	radical C	exo C	endo C	radical C
R1	0.801	−0.012	0.108	0.439	−0.007	0.094	0.222	−0.019	0.037	0.916
R2	4.663	−0.023	0.112	0.430	0.080	0.158	0.221	−0.021	0.044	0.888
R3	4.331	−0.019	0.123	0.461	0.086	0.158	0.235	−0.030	0.062	0.881
R4	0.812	−0.009	0.150	0.453	−0.015	0.103	0.228	−0.035	0.072	0.905
R5	4.155	−0.021	0.121	0.445	0.100	0.183	0.227	−0.026	0.053	0.892
R6	1.438	−0.014	0.083	0.398	−0.020	0.064	0.200	−0.019	0.042	0.730
R7	0.896	−0.010	0.132	0.464	0.021	0.120	0.237	−0.023	0.047	0.912
R8	1.552	−0.015	0.075	0.400	0.009	0.075	0.209	−0.013	0.029	0.735
R9	1.408	0.007	0.056	0.387	0.000	0.052	0.194	−0.009	0.030	0.732
R10	1.616	0.002	0.042	0.399	0.016	0.093	0.206	−0.007	0.019	0.736
R11	1.840	0.009	0.027	0.349	0.020	0.076	0.178	−0.007	0.019	0.727

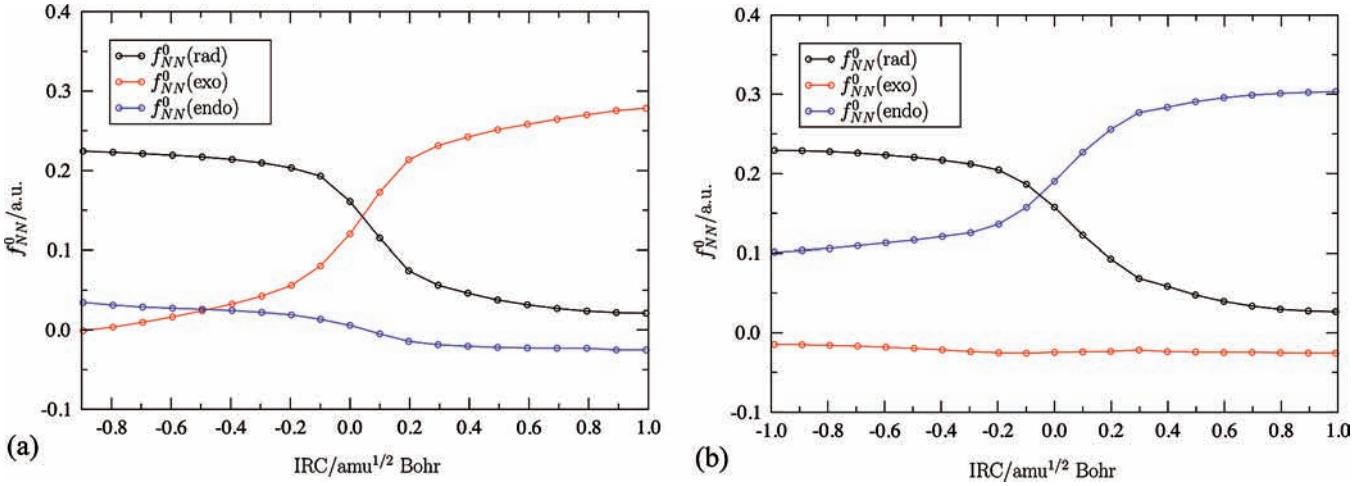

Figure 2. Evolution of the spin-polarized Fukui function for a radical attack f^0_{NN} on the radical center, exo and endo carbon atoms along the (a) endo-cyclization mode for radical R10 and (b) exo-cyclization mode of radical **R4**.

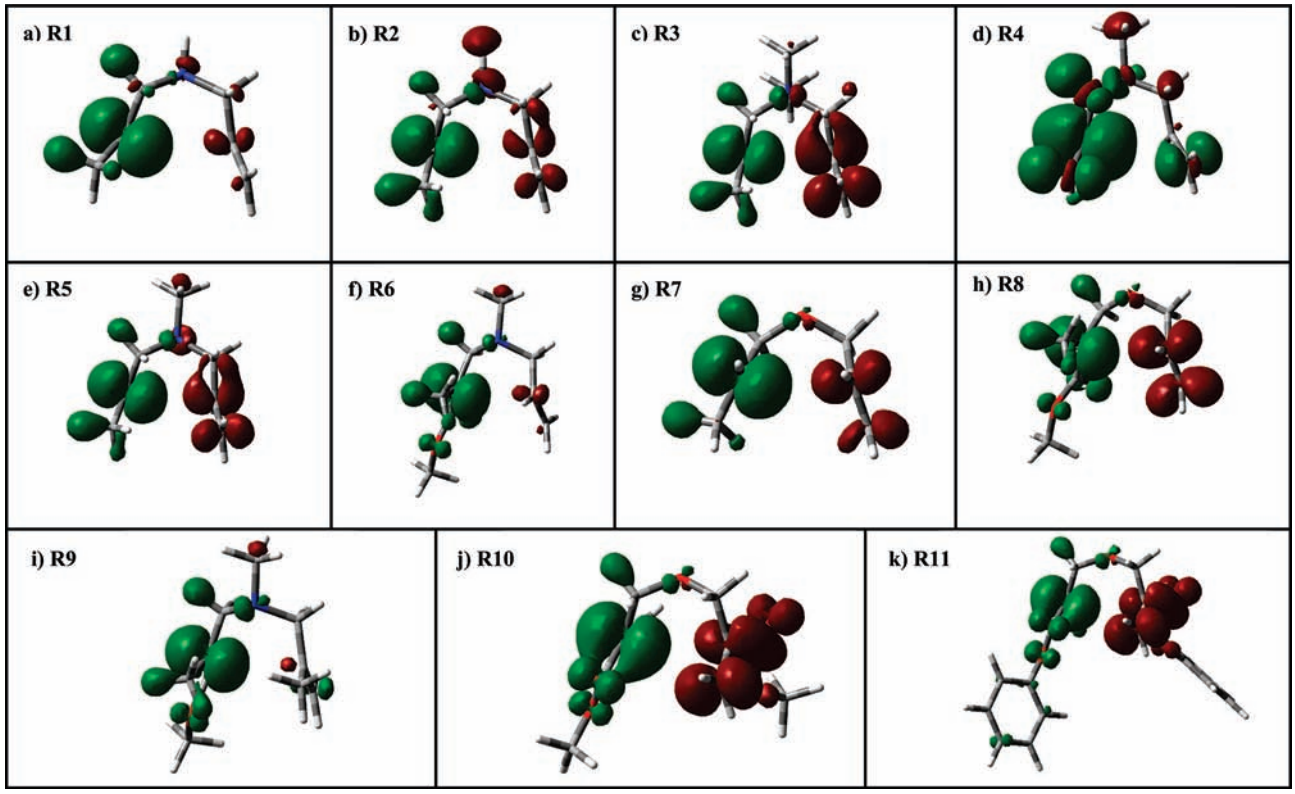

Figure 3. Spin-polarized dual descriptor $f^{(2)}_{\alpha\alpha\alpha}(\underline{r})$, as defined in eq 16, for all the radicals considered in this work (isosurface value = 0.0005).

between the radical carbon and the endo carbon of the endo transition state geometry. In the "exo TS for **R4**" the distance between the radical carbon and the exo carbon is 2.244 Å; in the "endo TS for **R4**", the distance between the radical carbon and the endo carbon is 2.320 Å. In the "reactive rotamer for **R4** (**R10**)" the distance between the radical carbon and the exo carbon is 2.924 Å (3.251 Å), and the distance between the radical carbon and the endo carbon is 3.604 Å (3.481 Å). Thus, in both cases, during the cyclization, starting from the reactive rotamer, it is easier to reach the exo transition state than the endo transition state. We have observed the same trend for the other radicals, as well.

Finally, we investigate whether the dual descriptor can specify the regioselectivity for the radical cyclization. Since the present cyclization corresponds to the transfer of an α electron from the α HOMO (mainly located on the radical center) to the α LUMO, the dual descriptor can be approximated by the difference of the densities of the α LUMO and HOMO densities.

$$f^{(2)}_{\alpha\alpha\alpha}(\underline{r}) = \left(\frac{\partial f_{\alpha\alpha}(\underline{r})}{\partial N_\alpha}\right)_v \approx |\psi^\alpha_{\mathrm{LUMO}}(\underline{r})|^2 - |\psi^\alpha_{\mathrm{HOMO}}(\underline{r})|^2 \tag{14a}$$

In Figure 3, we plotted the dual descriptors for all of the model radicals (isosurface value is 0.0005). For the radicals with a large number of heavy atoms (**R8**, **R10**, **R11**), the isosurface value 0.0005 is not large enough to visualize the differences between endo and exo carbons, so the dual descriptors of these radicals **R8**, **R10**, and **R11** are replotted with the isosurface value 0.004 in Figure 4.

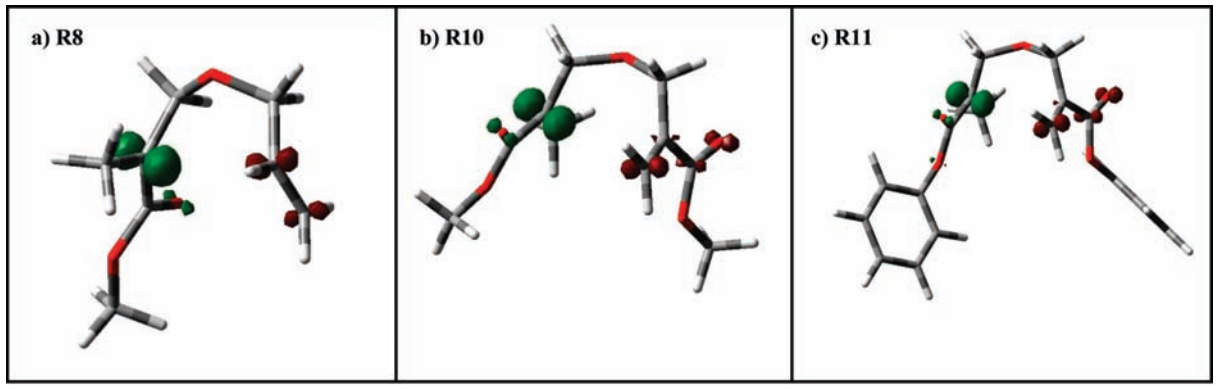

Figure 4. Spin-polarized dual descriptor $f^{(2)}_{\alpha\alpha\alpha}(\underline{r})$, as defined in eq 16, for all the radicals **R8**, **R10**, **R11** (isosurface value = 0.004).

For the four prototypical radicals considered in this work, both the radicals **R1** and **R4** show an exo regioselectivity in the cyclization, and **R10** and **R11** prefer the endo pathway. For **R1** in Figure 3a, the region of the dual descriptor is larger around the exo carbon than around the endo one. In addition, there is a favorable alignment between the quantity on the radical center (green) and the exo carbon (red). For the **R4** case in Figure 3d, the lobe on the exo carbon cannot be visualized with these iso values; however, the repulsive interaction between the radical and the endo carbon can be seen. When the iso values are decreased, a small, red region can be seen on the exo carbon. These results show that according to the dual descriptors, these two radicals undergo exo-cyclization, which is consistent with the experimental results. The same conclusions are reached for the other radicals, **R2**, **R3**, **R5**, **R6**, **R7**, and **R8**, that are experimentally observed to undergo exo-cyclization.

For **R10** and **R11**, in Figure 3j (or Figure 4b) and 3k (or Figure 4c), the dual descriptor region around the endo carbon is larger than the one around the exo carbon. There is a favorable interaction between the orbital on the radical center (green) and the endo carbon (red). These results show that **R10** and **R11** undergo endo-cyclization, which is again consistent with the experimental findings. It can thus be concluded that the spin-polarized dual descriptor, introduced in eq 14, captures the stereoelectronic effects determining the regioselectivity in these radical cyclizations. The only exception is **R9** in Figure 3i, which displays the endo reaction pathway and where the dual descriptor points to the exo carbon as the preferred carbon for cyclization. In this case, the observed regioselectivity is probably due to the combination of two effects: the large entropic favorability for the exo position (Table 1) and the large electrostatic contribution (Table 3).

4. Conclusions

Eleven representative radicals, **R1**−**R11**, were scrutinized to explore the regioselectivity in the cyclopolymerization reactions of diallyl monomers. The calculated activation barriers, activation enthalpies, and Gibb's free energies support the experimental trend that shows that **R1**−**R8** form five-membered ring structures and **R9**−**R11** form six-membered ring structures. The same observation holds for the entropies of activation, except for **R11**. The energy partitioning of the activation barriers shows that for the systems investigated, the regioselectivity cannot be explained by the steric effect, but that, instead, a nice linear relationship between the barrier differences and the electrostatic contributions can be established. The non-spin-polarized (f^0) and spin-polarized Fukui function (f^0_{NN}) values of the reactive rotamers, used as descriptors of the polar effect in these cyclizations, do not reproduce the experimental regioselectivity, since both favor the formation of the six-membered ring in all cases. Conversely, the spin densities, ρ_s, favor the five-membered ring structure. Examining the spin-polarized Fukui function along the reaction path has allowed us to observe the reactivities of the carbon atoms for the model radicals **R4** and **R10**. In both cases, the Fukui indices along the whole reaction pathway depict the regioselectivities. Finally, the dual descriptor $f^{(2)}(r)$ measuring stereoelectronic effects and computed in the framework of spin-polarized conceptual DFT has been found to explain the regioselectivity. The positive overlap between the radical center and the exo carbon for the radicals **R1**−**R8** and the positive overlap between the radical center and the endo carbon for the radicals **R10**−**R11** confirm the experimental findings. Radical **R9** is the only exception to the predicted reactivity based on dual descriptor analysis.

Acknowledgment. The computational resources used in this work were provided by the TUBITAK ULAKBIM High Performance Computing Center, Boğaziçi University Research Foundation (Project number: 07HB0503). The authors acknowledge the sixth framework project COSBIOM (FP6-2004-ACC-SSA-2.517991) for funding travel and lodging expenses. I.U., N.T., and V.A. gratefully acknowledge Professor Duygu Avcı for many interesting discussions and suggestions concerning free radical polymerization reactions. F.D.V. and F.D.P. acknowledge financial support from a Research Program of the Research Foundation−Flanders (FWO) (G.0464.06). F.D.P. and P.G. also acknowledge the Free University of Brussels (VUB) and the FWO for continuous support to their research group. P.W.A. acknowledges support from NSERC and the Canada Research Chairs.

References and Notes

(1) Zubov, V. P.; Kumar, M. V.; Masterova, M. N.; Kabanov, V. A. *J. Macromol. Sci.: Chem.* **1979**, *A13* (1), 111.
(2) (a) Matsumoto, A. *Prog. Polym. Sci.* **2001**, *26*, 189–257. (b) Harada, S.; Hasegawa, S. *Macromol. Chem. Rapid Commun.* **1984**, *5*, 27.
(3) Butler, G. B.; Bunch, R. L. *J. Am. Chem. Soc.* **1949**, *71*, 3120.
(4) Butler, G. B. *Cyclopolymerization and Cyclocopolymerization*; Marcel Dekker: New York, 1992.
(5) Butler, G. B.; Ingley, F. L. *J. Am. Chem. Soc.* **1951**, *72*, 894.
(6) Tüzün, N. S.; Aviyente, V. *J. Phys. Chem. A* **2002**, *106*, 8184–8190.
(7) Tüzün, N. S.; Aviyente, V. *Int. J. Quantum Chem.* **2007**, *107*, 894–906.
(8) Tüzün, N. S.; Aviyente, V.; Houk, K. N. *J. Org. Chem.* **2003**, *68*, 6369–6374.
(9) Tüzün, N. S.; Aviyente, V.; Houk, K. N. *J. Org. Chem.* **2002**, *67*, 5068–5075.
(10) Pinter, B.; De Proft, F.; Van Speybroeck, V.; Hemelsoet, K.; Waroquier, M.; Chamorro, E.; Veszpremi, T.; Geerlings, P. *J. Org. Chem.* **2007**, *72*, 348–356.

(11) Kodaira, T.; Liu, Q.-Q.; Satoyama, M.; Urushisaki, M.; Utsumi, H. *Polymer* **1999**, *40*, 6947–6954, and references therein.

(12) Pinter, B.; De Proft, F.; Van Speybroeck, V.; Hemelsoet, K.; Waroquier, M.; Chamorro, E.; Veszpremi, T.; Geerlings, P. *J. Org. Chem.* **2007**, *72*, 348–356.

(13) (a) Parr, R. G.; Yang, W. *Density Functional Theory of Atoms and Molecules*; Oxford University Press: New York, 1989. (b) Parr, R. G.; Yang, W. *Annu. Rev. Phys. Chem.* **1995**, *46*, 701. (c) Kohn, W.; Becke, A. D.; Parr, R. G. *J. Phys. Chem.* **1996**, *100*, 12974. (d) Geerlings, P.; De Proft, F.; Langenaeker, W. *Adv. Quantum Chem.* **1999**, *33*, 303. (e) Chermette, H. *J. Comput. Chem.* **1999**, *20*, 129. (f) Geerlings, P.; De Proft, F.; Langenaeker, W. *Chem. Rev.* **2003**, *103*, 1793. (g) Ayers, P. W.; Anderson, J. S. M.; Bartolotti, L. J. *Int. J. Quantum Chem.* **2005**, *101*, 520. (h) Liu, S. B. *Acta Phys. Chim. Sin.* **2009**, *25*, in press. (i) Geerlings, P.; De Proft, F. *Phys. Chem. Chem. Phys.* **2008**, *10*, 3028.

(14) Parr, R. G.; Yang, W. T. *J. Am. Chem. Soc.* **1984**, *106*, 4049.

(15) Ayers, P. W.; Levy, M. *Theor. Chem. Acc.* **2000**, *103*, 353.

(16) Perdew, J. P.; Parr, R. G.; Levy, M., Jr. *Phys. Rev. Lett.* **1982**, *49*, 1691.

(17) Ayers, P. W. *J. Math. Chem.* **2008**, *43*, 285.

(18) Morell, C.; Grand, A.; Toro-Labbe, A. *J. Phys. Chem. A* **2005**, *109*, 205.

(19) Ayers, P. W.; Morell, C.; De Proft, F.; Geerlings, P. *Chem.—Eur. J.* **2007**, *13*, 8240.

(20) Parr, R. G.; Von Szentpaly, L.; Liu, S. B. *J. Am. Chem. Soc.* **1999**, *121*, 1922.

(21) Chattaraj, P. K.; Sarkar, U.; Roy, D. R. *Chem. Rev.* **2006**, *106*, 2065.

(22) Parr, R. G.; Donnelly, R. A.; Levy, M.; Palke, W. E. *J. Chem. Phys.* **1978**, *68*, 3801.

(23) Parr, R. G.; Pearson, R. G. *J. Am. Chem. Soc.* **1983**, *105*, 7512.

(24) Pearson, R. G. *Chemical Hardness*; Wiley-VCH: Weinheim, Germany, 1997.

(25) Ayers, P. W. *Faraday Discuss.* **2007**, *135*, 161.

(26) (a) Galvan, M.; Vela, A.; Gazquez, J. L. *J. Phys. Chem.* **1988**, *92*, 6470. (b) Pérez, P.; Chamorro, E.; Ayers, P. W. *J. Chem. Phys.* **2008**, *124*, 204108. (c) Ghanty, T. K.; Ghosh, S. K. *J. Am. Chem. Soc.* **1994**, *116*, 3943.

(27) Garza, J.; Vargas, R.; Cedillo, A.; Galvan, M.; Chattaraj, P. K. *Theor. Chem. Acc.* **2006**, *115*, 257.

(28) Chamorro, E.; Pérez, P.; Duque, M.; De Proft, F.; Geerlings, P. *J. Chem. Phys.* **2008**, *129*, 064117.

(29) Liu, S. B. *J. Chem. Phys.* **2007**, *126*, 244103.

(30) (a) Nagy, A. *Chem. Phys. Lett.* **2007**, *449*, 212. (b) Liu, S. B. *J. Chem. Phys.* **2007**, *126*, 191107. (c) Liu, S. B.; Govind, N. *J. Phys. Chem. A* **2008**, *112*, 6690. (d) Liu, S. B.; Govind, N.; Pedersen, L. G. *J. Chem. Phys.* **2008**, *129*, 094104. (e) Nagy, A.; Liu, S. B. *Phys. Lett. A* **2008**, *372*, 1654. (f) Torrent-Sucarrat, M.; Liu, S. B.; De Proft, F. *J. Phys. Chem. A* **2009**, *113*, 3698. (g) Borgoo, A.; Jaque, P.; Toro-Labbé, A.; Van Alsenoy, C.; Geerlings, P. *Phys. Chem. Chem. Phys.* **2009**, *11*, 476.

(31) (a) Becke, A. D. *J. Chem. Phys.* **1993**, *98*, 5648. (b) Lee, C.; Yang, W.; Parr, R. G. *Phys. Rev. B* **1988**, *37*, 785. (c) Stephens, P. J.; Devlin, F. J.; Chabalowski, C. F.; Frisch, M. J. *J. Phys. Chem.* **1994**, *98*, 11623.

(32) For a detailed account on these types of basis sets, see, e.g.: (a) Hehre, W. J.; Radom, L.; von Raque Schleyer, P.; Pople, J. A. *Ab Initio Molecular Orbital Theory*; Wiley: New York, 1986.

(33) (a) Frisch, M. J. et al. Gaussian, Inc., Wallingford CT, 2004. (b) Frisch, M. J.; Trucks, G. W.; Schlegel, H. B.; Scuseria, G. E.; Robb, M. A.; Cheeseman, J. R.; Montgomery, J. A., Jr.; Vreven, T.; Kudin, K. N.; Burant, J. C.; Millam, J. M.; Iyengar, S. S.; Tomasi, J.; Barone, V.; Mennucci, B.; Cossi, M.; Scalmani, G.; Rega, N.; Petersson, G. A.; Nakatsuji, H.; Hada, M.; Ehara, M.; Toyota, K.; Fukuda, R.; Hasegawa, J.; Ishida, M.; Nakajima, T.; Honda, Y.; Kitao, O.; Nakai, H.; Klene, M.; Li, X.; Knox, J. E.; Hratchian, H. P.; Cross, J. B.; Bakken, V.; Adamo, C.; Jaramillo, J.; Gomperts, R.; Stratmann, R. E.; Yazyev, O.; Austin, A. J.; Cammi, R.; Pomelli, C.; Ochterski, J. W.; Ayala, P. Y.; Morokuma, K.; Voth, G. A.; Salvador, P.; Dannenberg, J. J.; Zakrzewski, V. G.; Dapprich, S.; Daniels, A. D.; Strain, M. C.; Farkas, O.; Malick, D. K.; Rabuck, A. D.; Raghavachari, K.; Foresman, J. B.; Ortiz, J. V.; Cui, Q.; Baboul, A. G.; Clifford, S.; Cioslowski, J.; Stefanov, B. B.; Liu, G.; Liashenko, A.; Piskorz, P.; Komaromi, I.; Martin, R. L.; Fox, D. J.; Keith, T.; Al-Laham, M. A.; Peng, C. Y.; Nanayakkara, A.; Challacombe, M.; Gill, P. M. W.; Johnson, B.; Chen, W.; Wong, M. W.; Gonzalez, C.; Pople, J. A. *Gaussian 03, Revision B.03*; Gaussian, Inc.: Wallingford, CT, 2004.

(34) (a) Reed, A. E.; Weinstock, R. B.; Weinhold, F. *J. Chem. Phys.* **1985**, *83*, 735. (b) Reed, A. E.; Weinhold, F. *J. Chem. Phys.* **1985**, *83*, 1736. (c) Reed, A. E.; Curtiss, L. A.; Weinhold, F. *Chem. Rev.* **1988**, *88*, 899.

(35) Tomasi, J.; Mennucci, B.; Cancès, E. *J. Mol. Struct. (THEOCHEM)* **1999**, *464*, 211–226.

(36) Cancès, M. T.; Mennucci, B.; Tomasi, J. *J. Chem. Phys.* **1997**, *107*, 3032–3041.

(37) Mennucci, B.; Tomasi, J. *J. Chem. Phys.* **1997**, *106*, 5151–5158.

(38) Mennucci, B.; Cancès, E.; Tomasi, J. *J. Phys. Chem. B* **1997**, *101*, 10506–10517.

(39) Kodaira, T.; Kasajima, N.; Urushisaki, M. *Polymer* **2000**, *41*, 2831–2837, and references therein.

(40) Johns, S. R.; Willing, R. I. *J. Macromol. Sci. Chem. A* **1976**, *10*, 875–891.

(41) Butler, G. B. *Cyclopolymerization and Cyclocopolymerization*; Marcel Dekker, Inc.: New York, 1992, p 54.

(42) Butler, G. B. *Cyclopolymerization and Cyclocopolymerization*; Marcel Dekker, Inc.: New York, 1992, p 71.

(43) Butler, G. B. *Cyclopolymerization and Cyclocopolymerization*; Marcel Dekker, Inc.: New York, 1992, p 257.

(44) Negi, Y.; Harada, S.; Ishizuka, O. *J. Polym. Sci., Part A-1* **1967**, 5.

(45) Beckwith, A. L. J. *Tetrahedron* **1981**, *37*, 3073–3075.

(46) Capon, B.; Rees, C. W. *Annu. Rep. Chem. Soc.* **1964**, *61*, 221.

(47) De Vleeschouwer, F.; Van Speybroeck, V.; Waroquier, M.; Geerlings, P.; De Proft, F. *Org. Lett.* **2007**, *9*, 2721.

JP903371B